Petroleum 4 (2018) 457–465

Contents lists available at ScienceDirect

Petroleum

journal homepage: www.keaipublishing.com/en/journals/petlm

Study on the fluid flow rule of five-cylinder plunger pump hydraulic end

Zhanghua Lian [a], Yang Liu [a], Tiejun Lin [a], Li Li [b], Zhongqing Lei [c], Chuanjun Han [a, *]

[a] State Key Laboratory of Oil and Gas Reservoir Geology and Exploitation, Southwest Petroleum University, 610500, PR China
[b] Institute of Technology, CNPC Xinjiang Oil Company, 834000, PR China
[c] Engineering Technology Research Institute, CNPC Bohai Drilling Engineering Company Limited, Tianjin, 300280, PR China

ARTICLE INFO

Article history:
Received 17 April 2017
Received in revised form
14 September 2017
Accepted 15 November 2017

Keywords:
Five-cylinder plunger pump
Pressure holding
Orifice jet
Vibration

ABSTRACT

The change of velocity and pressure of flow field in suction and discharge chamber of five-cylinder plunger pump obtained by CFD under maximum and minimum stroke, the results show that: when the stroke is 79 rpm, the internal of pump head will produce pressure holding, and the internal organization of pump head body will be in a fatigue state of high pressure for a long time. When the rotate angle is small, the peak velocity at the gap of valve disc and valve seat reaches 9.60 m/s, which is the orifice jet phenomenon. When the stroke is 299 rpm, the overall velocity curve is relatively stable, but the velocity of fluid flow through the pump head body is larger, and the maximum velocity reaches 18.72 m/s at the bottom corner of valve, it will produce the circumfluence and vortex discharge chamber at the same time, which will cause the increase of vibration of pump head body. So it should use proper punching gear in order to conducive to overall working life of pump.

1. Introduction

In order to effectively meet requirements for fracturing truck capacity, ultrahigh pressure, large displacement and intelligence in modern integrated fracturing unit construction as shown in Fig. 1, Xuping Zhao et al. put forward the development direction of new fracturing trucks in capacity, weight, energy conservation, emissions and consumption costs [1,2].

High pressure plunger pump is expensive, maintenance costs are very high in abroad, while domestic manufacturers are less than other developed country, failure of the hydraulic end often occurs in the fracturing pump as shown in Fig. 2, and some researches of mechanism and internal structure for reciprocating pump of hydraulic end has also been done at home and abroad:

Chuanjun Han et al. find it would produce vertex and counter flow when the flow went through the chamber, which is beneficial to optimizing designing and increased service life of the pump valve [3–7]. Qiming Yang, T. Henshaw et al. optimize 20CrMnTi under the condition of affecting wear, which supplies a guiding significance to research the new materials of wear-resisting in valves of the fracturing pump [8–13]. Faguang Jiang, P.J. Singh et al. obtain the characteristics of severe erosion and abrasion in the drilling pump valve by FLUENT. In addition, develop a new HP 1400 fracturing pump successfully through systemically theory study and structure analysis based on the reverse engineering technology, which offers a kind of effective method to study other similar products [14–19]. Gongxiang Zhong et al. choose support vector machine training feature sample data, and showed the fault recognition rate is about 95% and the results are accuracy and reliability [20–23]. Yongjun Hou et al. put forward a kind of triplex single-function reciprocating pump driven by linear motors, which developing new style reciprocating pump and designing its controlling system [24–26]. Y. Cengel, Zhidong Zhang et al. propose a fault diagnosis method of fluid end that combines the statistical indexes and neural network, which can be applied to engineering practice [27–29]. Herb et al. also consider the boundary of the flow field, they provide a certain basis for valve failure through the

* Corresponding author.
E-mail address: hanchuanjun@126.com (C. Han).
Peer review under responsibility of Southwest Petroleum University.

Production and Hosting by Elsevier on behalf of KeAi

https://doi.org/10.1016/j.petlm.2017.11.001

Fig. 1. Integrated fracturing unit.

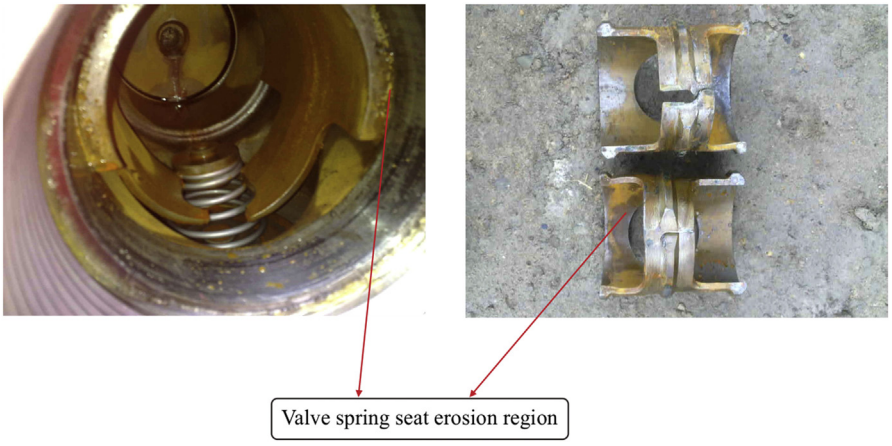

Fig. 2. The failure of the hydraulic end often occurs.

tribology theory, moreover some researches about the valve gap flow of variable section and non-Newtonian fluid in high shear with unsteady characteristics have been done [30–32].

The previous literature mainly aimed at analysis about flow of three cylinder pump, and there is little analysis research data of three-dimension flow of hydraulic end. This paper firstly does analysis for fluid flow of five cylinder plunger pump hydraulic end, constructs many kinds of precise models of transient flow field, and to study the rationality of channel structure by analyze flow field pressure and flow size and distribution.

2. Working principle of five cylinder plunger pump

Five-cylinder plunger pump belongs to volume pump, the periodic change of working chamber volume is produced by reciprocating motion of plunger in the hydraulic cylinder. Structurally, the working chamber is separated from the outside through the sealing device. In the process of working, mechanical energy of piston pump transmits directly into pressure energy of liquid [33, 34].

Fig. 3 is the working principle diagram of five cylinder, Fig. 3 (a) shows the crank OA rotating with uniform angular velocity of ω, when the crank rotating angle $\varphi = 0\sim\pi$, it is the suction stroke, the crank rotating angle $\varphi = \pi\sim2\pi$, it is the discharge stroke. When cross head is at the left of crank, crank is rotating along clockwise, Fig. 3 (b) is the diagram of rise and dropping process of suction valve and discharge valve of hydraulic end.

The movement of crosshead and piston is the same, so the movement of B in the center of crosshead pin can be indicated the movement of piston. We can see from Fig. 3, plunger displacement formula:

$$s \approx r\left(1 \mp \cos\varphi \pm \frac{\lambda}{2}\sin^2\varphi\right) \tag{1}$$

Plunger velocity formula:

$$u \approx \pm r\omega\left(\sin\varphi + \frac{\lambda}{2}\sin^2\varphi\right) \tag{2}$$

The valve lift distance formula:

$$h = \frac{A_1\omega r\sin\omega t}{\mu\pi d_1\sqrt{\frac{2(G+R)}{A_2\rho}}\sin\theta} \tag{3}$$

In the formula:

A_1—The cross sectional area of piston; A_2—Valve disc area; μ—The flow coefficient of valve, here is 1.12; ρ—Medium density; h—valve disc lift; ω—Crank angular velocity, R—spring force, 298 N; θ—The angle between the surface and the valve disc with the axis.

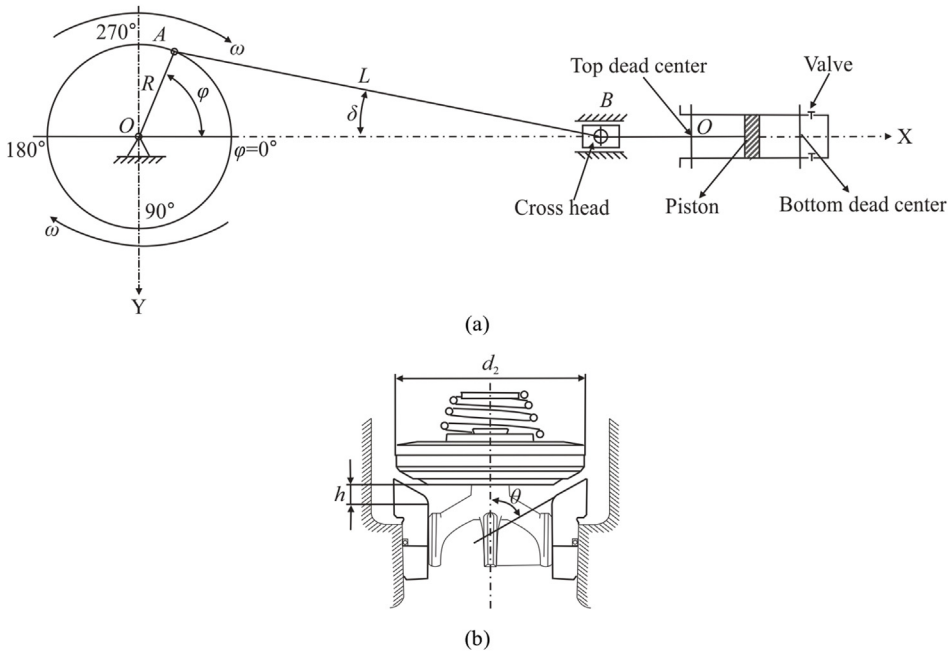

Fig. 3. The working principle of plunger pump.

3. Numerical calculation

3.1. Computational model

According to the structure design of five cylinder pump hydraulic end, and considering the practical numerical simulation, to establish the exact transient fluid model of the hydraulic end flow passage according to various conditions, including the fluid calculation model suction and discharge process of, select the transient model as the computational fluid domain, as shown follows in Fig. 4.

3.2. Boundary conditions of fluid field

From analysis of hydraulic end, it is known that the fluid was turbulent cylinder internal in suction and discharge process, and flow field of hydraulic end are complex, the parameters (flow pressure and velocity) are irregular changes continuously with time. Therefore, it is need to make the following assumptions for the numerical simulation of flow field [35, 36]:

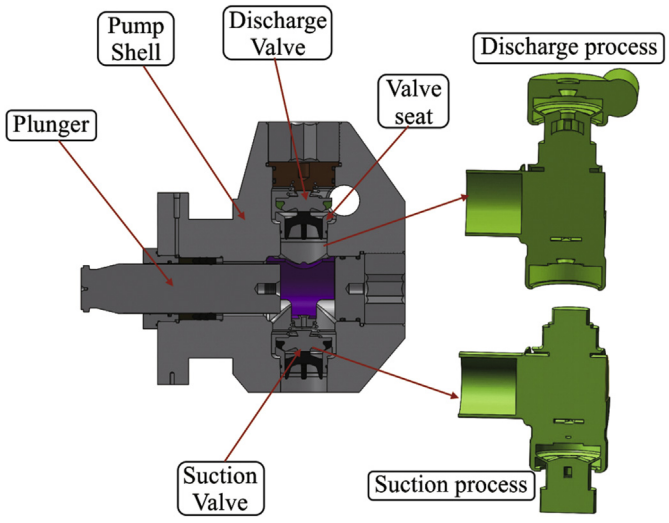

Fig. 4. The internal structure of hydraulic end and the fluid field model.

(1) Fluid as Newtonian Fluid (along with the velocity gradient change, dynamic viscosity μ unchanged)
(2) Through the calculation, the Reynolds number Re of the model far outweigh the critical Reynolds number Re (2000–3000), so the flow model state was mainly on the turbulent flow, which fulfilled $k-\varepsilon$ turbulence model.
(3) To solve discrete equations, Numerical calculation in common used the SIMPLE (Semi-Implicit Method for Pressure-Linked Equations) algorithm of the finite volume method.
(4) The wall boundary was no slip condition, namely $u_{wall}=0$, $v_{wall}=0$, $w_{wall}=0$, $k_{wall}=0$, $\varepsilon_{wall}=0$.
(5) Boundary condition of the model: In order to further explore the relationship between the valve internal flow velocity and pressure distribution and movement of the plunger pump, the parameters of suction process and discharge process under the maximal and the minimal stroke are obtained by calculating (generally, the maximum stroke is 299 rpm and the minimum stroke is 79 rpm), and the parameters values are shown in Tables 1 and 2.

4. Analysis of calculation results

4.1. Comparison of pressure changes in the suction process

It can be obtained the results from the simulation analysis of suctioning process under the maximum and the minimum stroke (Because of the paper space, only choose the pressure contours and velocity contours under three rotate angles) as shown in Fig. 5 and Fig. 6. With increase of the height of valve rising, the pressure in the suction chamber increases, and the increase rate is not large, it is at about 0.3 MPa. When the stroke is 79 rpm, the height is relatively small, and the fluid passes through the gap of valve and valve seat,

Table 1
The parameters of suction process.

Stroke n/rpm	Crank angle φ/°	Lift distance h/mm	Plunger velocity u/(m/s)	Plunger displacement s/m	Suction pressure P/MPa
79	15	0.789	0.231	4.120	0.3
	30	1.524	0.491	16.093	
	45	2.155	0.687	34.727	
	60	2.640	0.799	58.237	
	75	2.944	0.853	84.531	
	90	3.048	0.840	111.516	
299	15	2.980	0.979	4.120	0.3
	30	5.767	1.859	16.093	
	45	8.155	2.559	34.727	
	60	9.988	3.023	58.237	
	75	11.142	3.227	84.531	
	90	11.534	3.18	111.516	

Table 2
The parameters of discharge process.

Stroke n/rpm	Crank angle φ/°	Lift distance h/mm	Plunger velocity u/(m/s)	Plunger displacement s/m	Suction pressure P/MPa
79	195	0.829	0.177	2.743	105
	210	1.596	0.349	11.13	
	225	2.255	0.512	24.81	
	240	2.782	0.657	43.36	
	255	2.937	0.771	66.05	
	270	3.040	0.840	91.68	
299	195	3.135	0.668	2.743	40
	210	6.035	1.321	11.13	
	225	8.534	1.938	24.81	
	240	10.531	2.485	43.36	
	255	11.116	2.917	66.05	
	270	11.505	3.18	91.68	

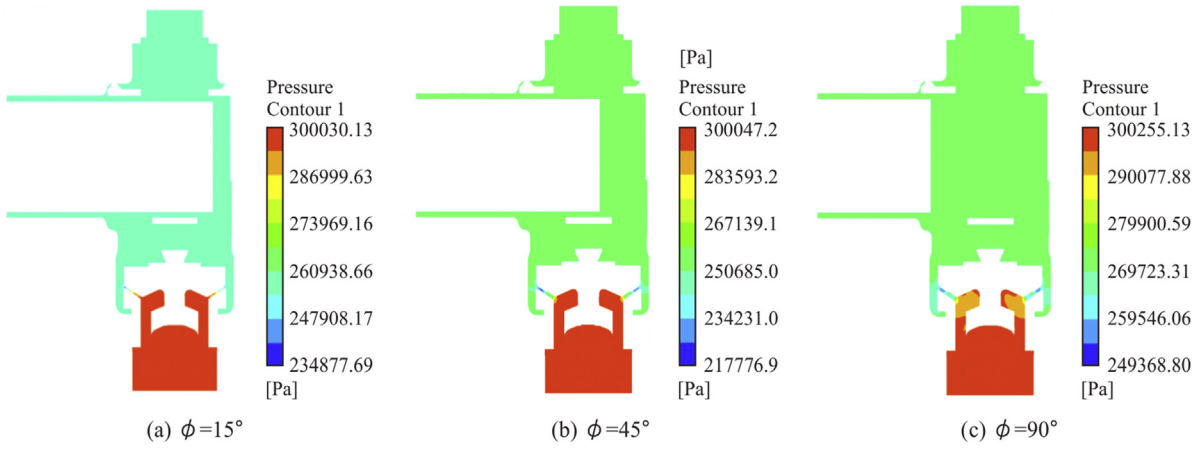

Fig. 5. Pressure contour in the suction process under79 rpm.

it will produce pressure-holding state. The pressure almost does not pass to upper chamber when the stroke is 79 rpm. When the stroke is 299 rpm, the height of valve rising is relatively large, it will release more pressure, the pressure will gradually spread to the upper chamber.

4.2. Comparison of velocity changes in the suction process

From the velocity vector diagram under the maximum and the minimum stroke as shown in Fig. 7 and Fig. 8, it can be found that the larger velocity of fluid is concentrated in the gap region of valve seat and valve, and the height of valve rising is bigger, the velocity through the valve gap increases. When the stroke is 79 rpm, the smaller the angle, the smaller the height of lifting is, the velocity of fluid flow in the suction chamber is also small. At this time, the velocity basically do not change much at the same time, and the maximum velocity is not become large with increase of opening. When the stroke is 299 rpm, with the rotation angle increasing, the height of rising is larger, the velocity of fluid flow in the suction chamber is also large and relatively higher in the suction chamber

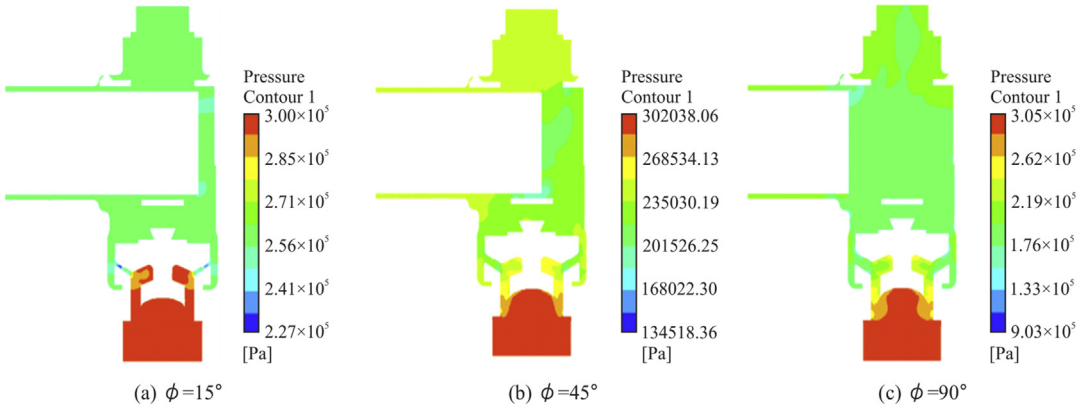

Fig. 6. Pressure contour in the suction process under 299 rpm.

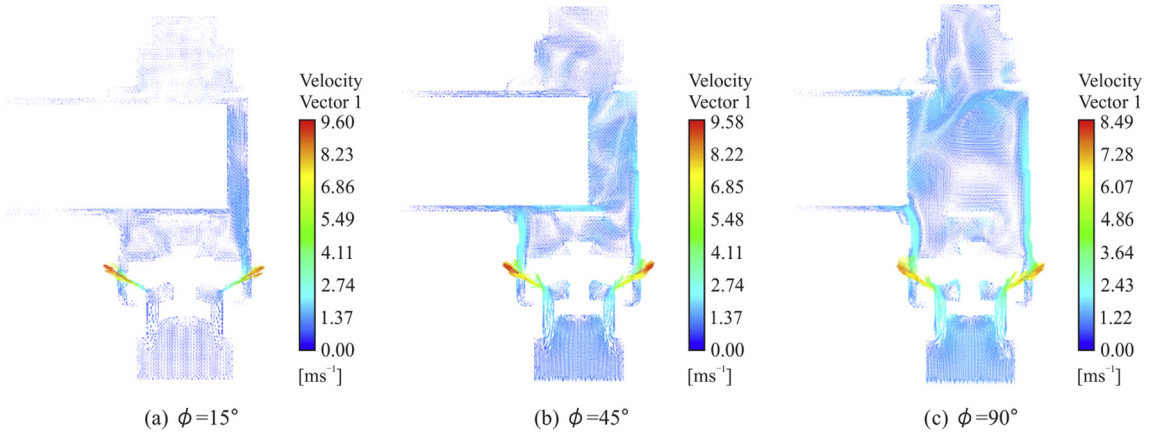

Fig. 7. Velocity vector diagram under 79 rpm.

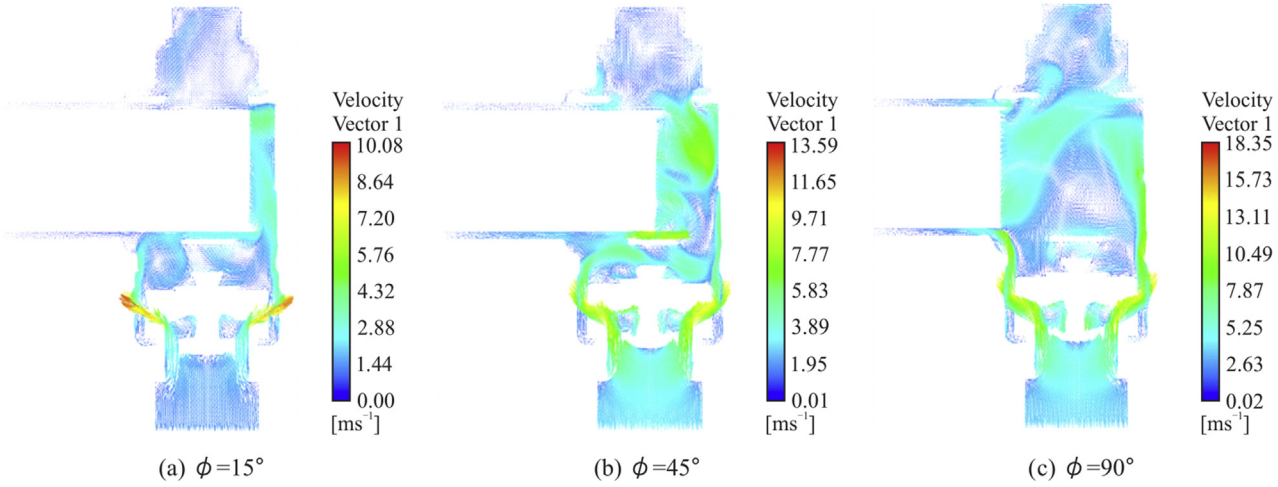

Fig. 8. Velocity vector diagram under 299 rpm.

at the same time. The maximum velocity will be increase with the opening increasing, and the maximum velocity reaches 16.5 m/s, in addition, the fluid flowing through the internal cavity, a part of vortex and circumfluence will be produced, therefore, the fluid has some impact on the suction chamber under the maximum stroke.

From Fig. 9, it can be obtained: when the stroke is constant, the overall velocity of flow field in the suction chamber will increase with angle increasing; when the stroke is 79 rpm, the velocity changes in a range of 0.2–9.5 m/s, although the angle is small at this time, for example, when the rotate angle is ø = 15°, the peak

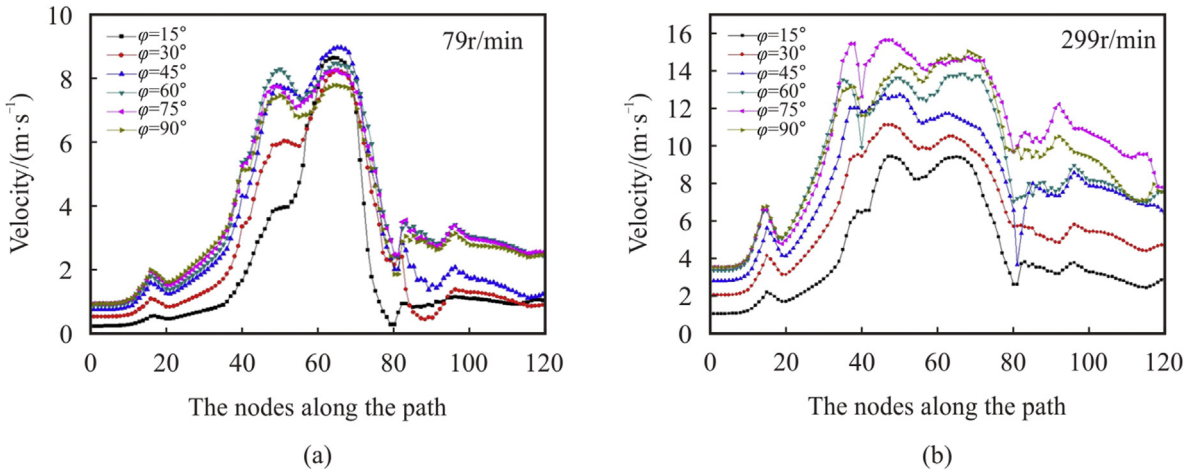

Fig. 9. Velocity curve of fluid in the suction chamber under 79 rpm and 299 rpm.

velocity changes greatly. When the stroke is 299 rpm, the overall velocity curve is relatively stable, the velocity changes in a range of 1.1–16 m/s, the velocity is mutation at the small region. It can be found the velocity of outlet position is larger than the entrance in the process of inhalation/suctioning.

4.3. Comparison of pressure changes in the discharge process

It can be obtained the results from the simulation analysis of discharging process under the maximum and the minimum stroke as shown in Fig. 10 and Fig. 11. With the increase of height, pressure in the discharge chamber increases, and the increase rate of

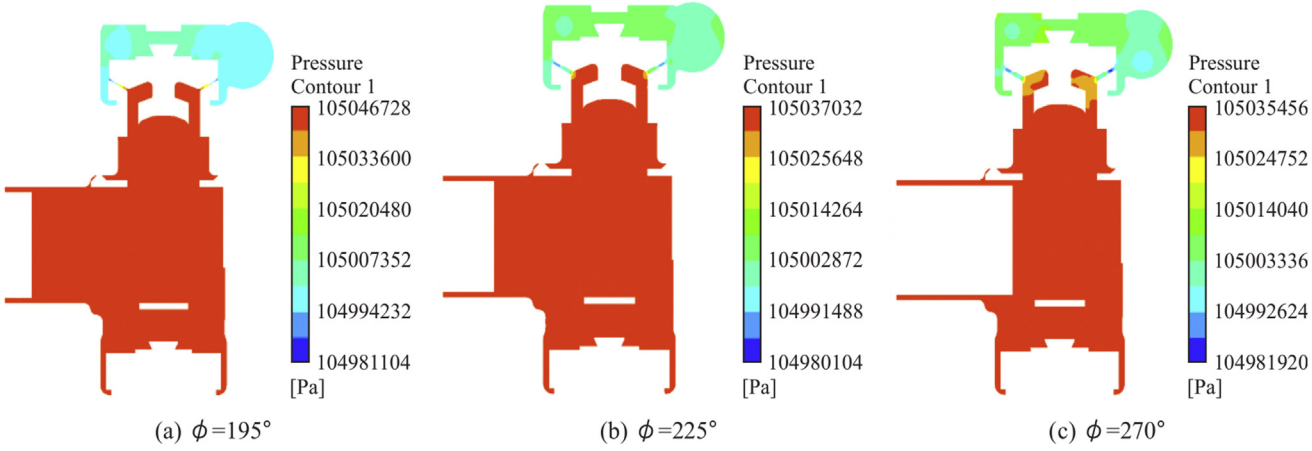

Fig. 10. Pressure contour in the discharge process under79 rpm.

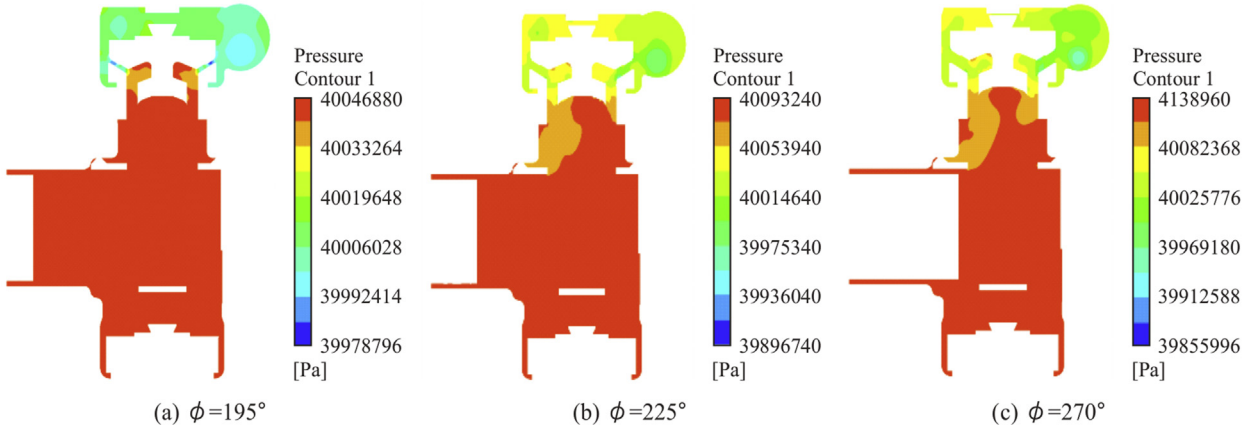

Fig. 11. Pressure contour in the discharge process under 299 rpm.

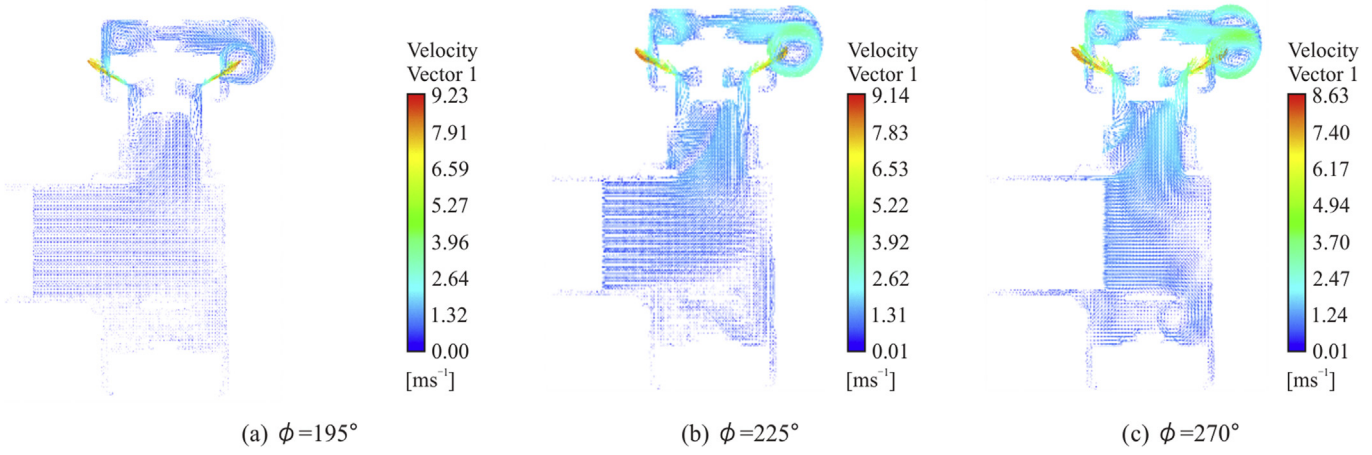

Fig. 12. The velocity vector diagram under 79 rpm.

pressure is not large. When the stroke is 79 rpm, the height is relatively small, when the fluid passes through the gap of valve and valve seat, it will also produce pressure-holding state, pressure almost do not pass to the upper outlet, when the stroke is 299 rpm, the height is relatively higher, it will release more pressure, the pressure will gradually spread to the upper outlet.

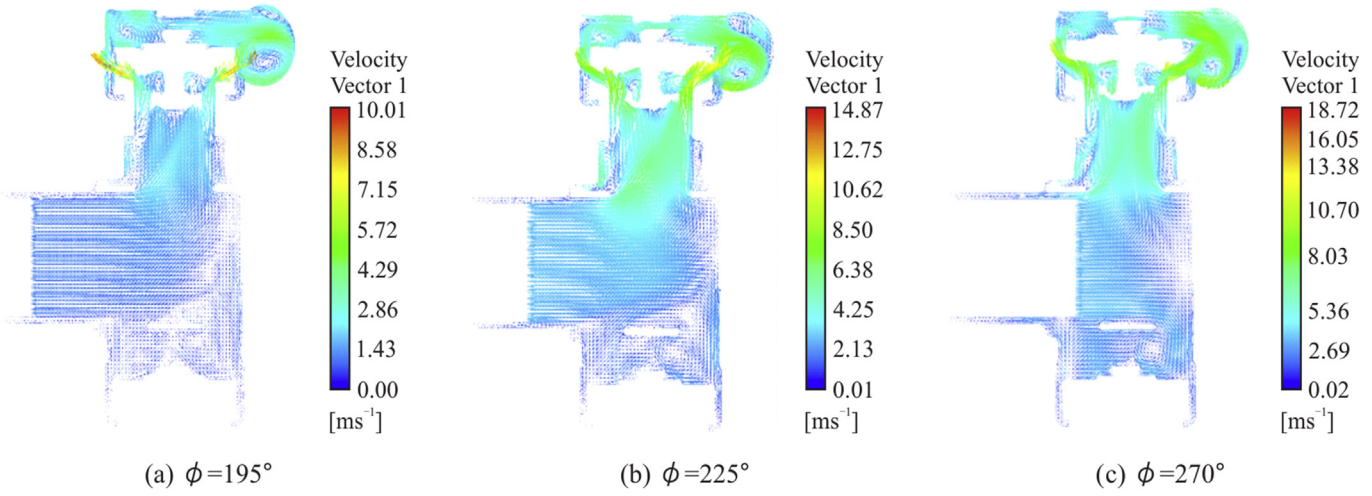

Fig. 13. The velocity vector diagram under 299 rpm.

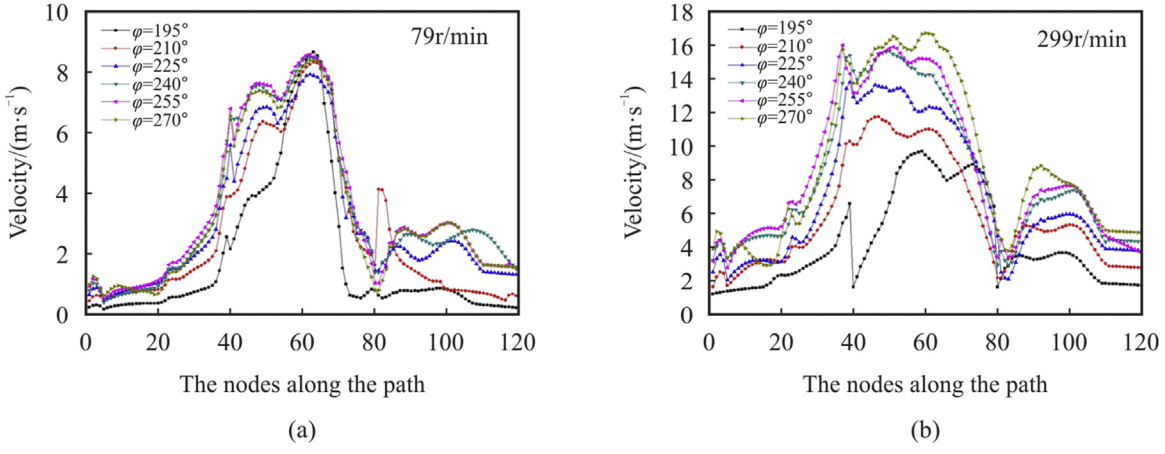

Fig. 14. Velocity curve of fluid in the discharge chamber under 79 rpm and 299 rpm.

4.4. Comparison of velocity changes in the discharge process

From the velocity vector diagram under the maximum and the minimum stroke as shown in Fig. 12 and Fig. 13, it can be found the larger velocity of fluid are concentrated in the gap region of valve seat and valve disc. And the height of valve rising is bigger, the smaller the angle, fluid flow in the discharge chamber is also small. Basically the fluid velocity does not change much, the maximum velocity does not increase with the opening increasing. In addition, the velocity of fluid flow through the valve gap increases, the velocity of fluid flow is larger at the valve gap and discharge holes. When the stroke is 79 rpm, the smaller the rotate angle, the smaller the height of valve rising is, the velocity of fluid flow in the discharge chamber is also small. The velocity of fluid flow basically does not change much at the same time, the maximum velocity does not increase with the opening increasing. When the rotate angle is $\varnothing = 15^{\circ}$, the larger velocity will appear in the gap of valve and valve seat, and the maximum velocity reaches 9.23 m/s. When the stroke is 299 rpm, with the rotation angle increasing, the height of valve rising is larger, fluid velocity is relatively higher in the discharge chamber at the same time. The maximum velocity will be increase with the opening increasing, and the maximum velocity reaches 18.72 m/s. In addition, a part of vortex and circumfluence appearance when the fluid flowing through the internal cavity, therefore, fluid has some impact on the discharge chamber under the maximum stroke.

From Fig. 14, it can be obtained: when the stroke is constant, the overall velocity of flow field in the discharge chamber will increase with rotate angle increasing. When the stroke is 79 rpm, the velocity of fluid flow changes in a range of 0.25–9.20 m/s, although small angle at this time. For example, when the rotate angle is $\varnothing = 195^{\circ}$, but its velocity change is large, the peak changes greatly. When the stroke is 299 rpm, the overall velocity curve is relatively stable, the velocity changes in a range of 1.12–17.1 m/s. The velocity of fluid flow is mutation at the small region, when rotate is $\varnothing = 270^{\circ}$, the maximum velocity appearances. At the same stroke and rotate angle, the velocity of fluid flow increases gradually and then gradually becomes smaller along the flow path of fluid. In the process of discharge process, it can be found the velocity of fluid flow at the plunger and outlet is very small, the velocity of outlet position is larger than the entrance.

5. Conclusions

Construct the internal flow model of hydraulic end precisely in this paper, and the fluid velocity and pressure contours obtained by the calculation of CFD under the maximum and minimum stroke respectively, the result showed that:

(1) When the stroke is constant under the maximum and minimum stroke, flow velocity will increase with increasing angle in suction and discharge process, the velocity of flow increases gradually and then decreases gradually at the same stroke and rotate angle.
(2) When the stroke is 79 rpm, although the average velocity of fluid flow into the suction chamber and the discharge chamber is small, the internal of pump head will produce pressure-holding.
(3) The gap of valve and valve seat is approximate micro hole, and the maximum velocity is very large in the at the bottom corner of valve, the sealing ring is easy to tear so that it causes leakage, especially when the stroke is 299 rpm, the fluid average velocity is too large, which will cause erosion of the cavity parts.
(4) When the stroke is larger, the fluid go into discharge chamber internal will produce the circumfluence and vortex, it will cause vibration of pump head body, it will damage the inner wall of the discharge chamber under the action for a long time.

Acknowledgements

The authors are grateful to the support from the National Natural Science Foundation of China No.51574198 and No.5157041475), Research Fund for the Doctoral Program of Higher Education of China (No.20135121110005).

References

[1] Zhao Xuping, Li Zhibo, et al., Research and development of fracturing truck, NGO 33 (5) (2015) 56–58.
[2] W. Milton Roy, Multi-purpose mud pump, World Pumps 412 (1) (2001) 7–9.
[3] Han Chuanjun, Liu Yang, et al., Studying on failure mechanism of pump valve of triplex plunger pump based on CFD, China Petrol. Mach. 39 (2) (2001) 9–11.
[4] Fansen Konga, Ruheng Chen, A combined method for triplex pump fault diagnosis based on wavelet transform, fuzzy logic and neuro-network, Mech. Syst. Signal Process. 18 (2004) 161–168.
[5] Vimal Chand, Sontake, Vilas R. Kalamkar, Solar photovoltaic water pumping system-A comprehensive review, Renew. Sustain. Energy Rev. 59 (2016) 1038–1067.
[6] M. Fernando, Tello Oquendo, et al., Performance of a scroll compressor with vapor injection and two-stage reciprocating compressor operating under extreme conditions, Int. J. Refrig. 63 (2016) 171–183.
[7] S.D. Able, Reciprocating pump acceleration head, in: Proceedings of ASME FEDSM01-2001 ASME Fluids Engineering Division Summer Meeting, New Orleans, USA, 2001, pp. 1–7.
[8] Yang Qiming, et al., Resisting wear property research of the material of new type fracturing pump valve, J. Southwest Pet. Inst. 32 (6) (2001) 73–76.
[9] T. Henshaw, Power pump valve dynamics-a study of the velocity and pressure distribution in outward-flow bevel face and flat-face power pump valves, in: Proceedings of 25th International, Magnolia Texas, 2009, pp. 23–32.
[10] J.J. Rudolf, T.R. Heidrick, B.A. Fleck, V.S.V. Rajan, Optimum design parameters for reciprocating pumps used in natural gas wells, J. Energy Resour. Technol. 127 (2005) 285–292.
[11] Boru Jia, Andrew Smallbone, et al., Design and simulation of a two- or four-stroke free-piston engine generator for range extender applications, Energy Convers. Manag. 111 (2016) 289–298.
[12] Lokesh Paradeshi, M. Srinivas, S. Jayaraj, Parametric studies of a simple direct expansion solar assisted heat pump operating in a hot and humid, Environ. Energy Procedia 90 (2016) 635–644.
[13] Gunnar Latz, Olof Erlandsson, et al., Performance analysis of a reciprocating piston expander and a plate type exhaust gas recirculation boiler in a water-based rankine cycle for heat recovery from a heavy duty diesel engine, Energies 9 (2016) 495–513.
[14] J.I.A.N.G. Faguang, et al., The application of reverse engineering technology in research and manufacturing in 1400 Fracturing pump, J. SW Petrol. Univ. 29 (3) (2007) 139–141.
[15] P.J. Singh, N.K. Madavan, Complete analysis and simulation of reciprocating pumps including system piping, in: Proceedings of the Fourth International Pump Symposium, Texas, USA, 1987, pp. 55–74.
[16] Y.A.N.G. Guoan, et al., Compute and analysis of the flow field in the play of the drilling pump valve based on the simulation by FLUENT, Oil Field Equip. 37 (3) (2008) 41–44.
[17] D.N. Johnston, Numerical modelling of reciprocating pumps with self-acting valves, Proceedings of the Institution of Mechanical Engineers, Part I, J. Syst. Control Eng. 205 (1991) 87–96.
[18] Yeng-Yung Tsui, Shiue-Lin Lu, Evaluation of the performance of a valueless micropump by CFD and lumped system analyses, Sensor. Actuator. 148 (1) (2008) 138–148.
[19] J.J. Rudolf, T.R. Heidrick, B.A. Fleck, V.S.V. Rajan, Optimum design parameters for reciprocating pumps used in natural gas wells, J. Energy Resour. Technol. 127 (2005) 285–292.
[20] Zhong Gongxiang, Zhang Yang, et al., A fault diagnosis method based indicator diagram for reciprocating pump hydraulic end, Mach. Des. Res. 31 (5) (2015) 172–176.
[21] Y. Wang, F Y, Z G, Finite element model of erosive wear on ductile and brittle materials, Wear 5–6 (265) (2008) 871–878.
[22] John Vande Voorde, Jan Vierendeels, Erik Dick, Flow simulations in rotary volumetric pumps and compressors with the fictitious domain method, J. Comput. Appl. Math. 168 (2004) 491–499.
[23] M T, Progress towards the optimization of a mechanical oscillator flowmeter, Flow Meas. Instrum. 1 (14) (2003) 13–22.

[24] G. Ma, Q. Chai, Y. Jiang, Experimental investigation of air source heat pump for cold regions, Int. J. Refrig. 26 (2003) 12–18.
[25] Hou Yongjun, et al., The research on motion characteristic of triplex single-function reciprocating pump driven by linear motors, J. SW Petrol. Univ. 31 (5) (2009) 163–166.
[26] C. Feng, Kai Shouguo, X. Ziwen, S. Pengcheng, Investigation of the heat pump water heater using economizer vapor injection system and mixture of R22/R600a, Int. J. Refrig. 32 (2009) 509–514.
[27] Y. Cengel, J. Cimbala, Fluid Mechanics: Fundamentals and Applications, third ed., McGraw-Hill, New York, USA, 2013.
[28] Zhang Zhidong, et al., Study on fault diagnosis technology for fluid end of drilling pump, J. SW Petrol. Univ. 37 (5) (2015) 168–172.
[29] T. Henshaw, Power pump valve dynamics-a study of the velocity and pressure distribution in outward-flow bevel face and flat-face power pump valves, in: Proceedings of 25th International, Magnolia Texas, 2009, pp. 23–32.
[30] Herb Harts home C J B W, Ferro Fluid-based Microchip Pump and Valve, Elsevier, Sensor. Actuator. (99) (2004) 592–600.
[31] Pei Junfeng, Zhang Siwei, Qi Mingxia, et al., A new method for fault diagnosis of fluid end in drilling pump, Acta Pet. Sin. 30 (4) (2009) 617–620.
[32] R. Amirante, G. Del Vescovo, A. Lippolis, Evaluation of the flow forces on an open center directional control valve by means of a computational fluid dynamic analysis, Energy Convers. Manag. 47 (13–14) (2006) 1748–1760.
[33] U. Adolph, Berechnung des Arbeitsspiels selbsttatiger Ventile schnellaufender Kolbenpumpen, Maschinenbau 17 (4) (1968) 189–193.
[34] Wan Banglie, Li Jizhi, et al., Petroleum Engineering Fluid Machinery, Petroleum Industry Press, Beijing, 1998.
[35] Wang Fujun, Analysis for Computational Fluid Dynamics, Tsinghua University Press, Beijing, 2004.
[36] Li Wanping, Computational Fluid Dynamics, Huazhong University of Science and Technology Press, Wuhan, 2004.